

Revisiting ant colony algorithms to seismic faults detection

W.Maciel¹ C.Vasconcelos² P.Silva¹ M.Gattass¹

1- Pontifícia Universidade Católica do Rio de Janeiro - Tecgraf Institute
Marquês de São Vicente, 225, Gávea, Rio de Janeiro - Brazil

2- Universidade Federal Fluminense - Department of Computer Science
Lara Vilela, 126, São Domingos, Niterói - Brazil

Abstract.

Seismic fault extracting is a time consuming task that can be aided by image enhancement of fault areas. The recent literature addresses this task by using ant colony optimization (ACO) algorithms to highlight the fault edges. This work proposes improvements to current state of the art methods by revisiting and/or reincorporating classic aspects of ACO, such as ant distribution, pheromone evaporation and deposition, not previously considered in this seismic fault enhancement scenario. The proposed approach arrives at good results presenting images with little noise and great localization of fault edges.

1 Introduction

A representation of the Earth's crust can be recovered by recording the signal generated by reflections of acoustic waves against its layers. The seismic amplitude volume is produced as the result of this process, known as seismic data acquisition, where time is the vertical coordinate that grows downwards, and the other dimensions are called inline and crossline. Each unidimensional sequence of values in the time dimension, defined as a trace, denotes the amplitudes of the reflecting acoustic waves. Figure 1(a) presents a sample of a seismic data.

A sequence of peaks (or valleys) in the amplitude across adjacent traces is called a horizon. Horizons are important structures to be mapped in seismic data because they represent the interface between layers of different materials. However the crust may have strong discontinuities across multiple horizons, such as the one seen on Figure 1(b), which displays a clear rip. These structures are called seismic faults and demand great effort to be mapped by hand. To aid geologists, many different image attributes may be used to visually highlight fault areas, as seen of Figure 1(c). However, these fault attributes often produce much noise and may not be sufficient for a clear fault edge delineation.

In this work, we address the task of seismic fault attribute enhancement as an ant colony optimization problem motivated by the good results presented by the recent literature. We propose revisiting classic formulations of ACO algorithms, such as ant distribution and pheromone evaporation and deposition, to further improve the method presented by Zhao *et al.* [1] by reincorporating them into our pipeline. Our contributions, detailed in Section 3, resulted in cleaner and sharper fault edges as illustrated and discussed in Section 4.

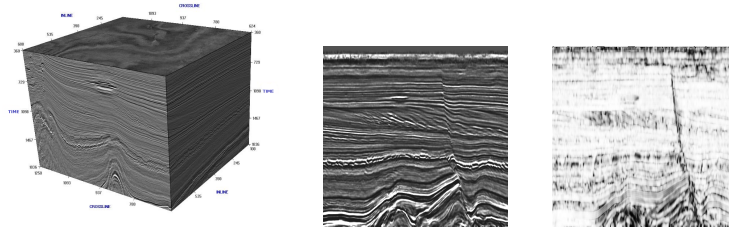


Fig. 1: Seismic amplitude volume, slice and attribute in order.

2 Related Works

Ant colony optimization (ACO) is a swarm intelligence algorithm inspired by the foraging behavior of ants in nature. Each ant has a very narrow view of the whole scope of the problem, as well as a limited set of actions it can perform. However, the interaction of their behavior with that of other ants creates an emergent intelligence for the colony as a whole.

Additionally, in an application scenario closer to our work, ant colony optimization algorithms has been used for fault attribute enhancement in seismic images. Pedersen *et al.* [2, 3] use the behavior of the ants for suppressing noise and Zhao *et al.* [1] uses a directional field to guide the ants through the image.

The contributions of our proposal, when compared to the related works cited above, are explained in further detail in the next sections.

3 Proposed Method

Our method for fault enhancement in seismic slices investigates the benefits of including classic ACO aspects to the method proposed by Zhao *et al.* [1], such as ant distribution and pheromone evaporation and deposition.

3.1 Initialization

The goal of the initialization phase is to prepare the image for a smoother tracking of the ants and define the initial states of the simulation. More specifically, this phase covers the normalization, smoothing, agent distribution and initial pheromone distribution procedures.

Different seismic attributes have different values associated with fault areas. Therefore, the fault attribute slice is normalized as to contain values ranging only between 0.0 and 1.0. However, a simple linear normalization may eliminate too much information if the attribute image has any outlier values. To address this issue, we eliminate outliers by clipping the maximum and minimum values of the image to n standard deviations. In order to eliminate some of the noise and smooth out strong variations in the attribute value, we use a low pass filter.

The initial position of the ants is a key variable to determine the quality of the final result. On the one hand, if we have too many ants spawning far away

from the fault areas, they will generate noise. On the other, excess concentration of the ants on main fault areas may cause them to ignore other small ones.

Therefore, we used a probabilistic approach as $P_i^k = (\eta_i)(\sum_{j \in I} \eta_j)^{-1}$, where P_i^k is the probability of an ant k to spawn on pixel i , I is the universe of pixels in the image and η_j is the value of the fault attribute on pixel j .

Additionally, in order to ensure a good balance between coverage and concentration, we propose using P_i^k in combination with the approach presented by Machado *et al.* [4]. In it, the initial number of ants, N , is divided evenly among three scales of gamma correction: $\gamma = 0.5, 1$ and 1.5 .

The initialization of pheromone values to a value E greater than zero is essential, because, otherwise, the ants would never start the search. Moreover, in our method, the same value used for the initialization is used to define a lower limit for the concentration of pheromone in every pixel. Our goal is to stop pixels from being eliminated from the search if they reach a zero valued pheromone.

3.2 Directional Field

After the seismic attribute image is treated, we use the method described by Bazen *et al.* [5] to compute a directional field alongside a related consistency field. These will be used to guide the ants during the tracking process.

The directions pointed by this field are the directions perpendicular to the gradient *i.e.* parallel to the ridge direction. This field is used to decide where the field of vision of the ants will be centered. The direction v_2 of each pixel is the smallest eigenvector of the autocovariance matrix C_G .

However, not all directions can be trusted. Therefore, a consistency field is created, which assigns a value Coh to how much the direction associated with a pixel agrees with the directions associated with its neighbors' pixels. It can be computed as $Coh = (\sqrt{(G_{xx} - G_{yy})^2 + 4G_{xy}})(G_{xx} + G_{yy})^{-1}$.

The consistency map binarization generates a consistency mask, which will delineate exactly which pixels can be trusted. In order to achieve more smoothed areas and eliminate some of the noise in the mask, the binary image undergoes two classical morphological treatments known as *opening* and *closing*.

3.3 Transition Rules

The transition rules dictate the behavior of the ants during the process. In summary, the transition of an ant k to a pixel i is given by a probabilistic function (1), where pixels with higher attractiveness have higher probabilities of being chosen as destination.

Each ant has a limited field of view, within the area of a slice of circle centered on the ant, pointing in the direction given by the directional field.

An ant's movement from a pixel to another, also known as transition, is a probabilistic event which occurs once per turn. Each ant, when its turn comes, checks which pixels can it move to and chooses its destination based on the amount of pheromone and on the value of the seismic attribute of the candidates.

P_{ij}^k , given by equation (1), is the probability of an ant k move from pixel i to pixel j . τ_j is the amount of pheromone on pixel j ; η_j is the value of the seismic attribute in j ; α and β are the weighting factors given to τ_j e η_j respectively.

$$P_{ij}^k = \frac{\tau_j^\alpha \eta_j^\beta}{\sum_{r \in \mathcal{V}_i^k} \tau_r^\alpha \eta_r^\beta} \quad (1)$$

Every turn, each ant picks a destination among the visible pixels. The location is stored in the ant's memory, so this pixel won't be visited again by the same ant. The ant is terminated when the number of pixels stored is bigger than a constant L , which is limited for memory and performance reasons.

It is highly likely that the destination is not adjacent to the origin. Because of this, to avoid having discontinuities, we use Bresenham's [6] line rasterization algorithm to find the pixels between destination and origin. These pixels, are treated as visited and are also added to the ant's memory.

To determine whether an ant is terminated or stays alive, we check the consistency of the current pixel, the direction pointed by the directional field and which pixels have already been visited.

Every time an ant steps onto a pixel outside of the consistency mask, it increments a counter L_{err} . When this counter reaches a threshold, the ant is terminated. Also, when the directional field is being calculated, it is possible that some patches of the image have the same pixel value, which would cause the directional field to be null, any ant that finds itself in one of these pixels is terminated. Additionally, if for any reason, an ant finds out that all the pixel it can see were already visited, it is also terminated.

It is important to remember that when we say that an ant is terminated, it is, in reality, relocated to a new pixel and it has its memory erased, which causes the algorithm to always be working with the same number of ants.

3.4 Pheromone Update

The pheromone update runs after the ants take each step. This procedure can be divided in two parts, evaporation and deposition of pheromone by the ants.

After each step, the pheromone concentration in every pixel is reduced. This process simulates the evaporation that would occur in nature by reducing pheromone in pixels less visited pixels, making them even less attractive to other ants. The evaporation is given as $\tau_i^t = \tau_i^{t-1}(1 - h)$, where τ_i^t is the pheromone concentration on pixel i during step t , and h is the evaporation rate.

The deposition of pheromone occurs right after the evaporation phase. In this moment, all ants that have been terminated in this iteration deposit an amount of pheromone equals to τ_k on top of every pixel in their memory. The value of τ_k is proportional to the euclidean distance d_{ij} between the first i and the final j point in the path. This behavior is described as $\tau_k = d_{ij}T$, where T is the pheromone constant which is used to moderate the amount of pheromone deposited.

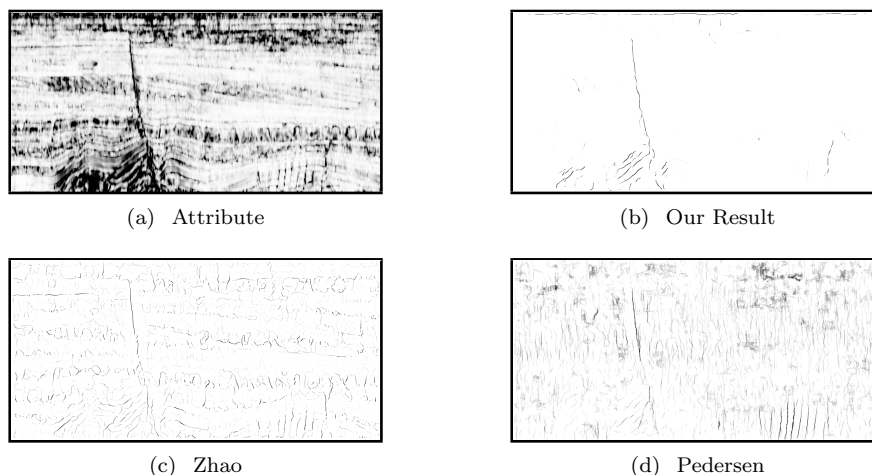


Fig. 2: F3Block's inline 279

3.5 Post Processing

The pheromone map goes through a post processing phase. Firstly, the image is normalized, then, its gamma factor is adjusted in order to suppress noise, in low intensity areas, and enhance areas where the intensity is high. After that, the resulting image is input to an edge thinning algorithm. The method used is the one presented by Canny [7], which uses non-maximum suppression.

4 Results

Next, we present two examples of the results obtained by our proposal along two other results from the works of Zhao *et al.* [1] and Pedersen *et al.* [2, 3].

The input images are displayed by Figures 2(a) and 3(a), which were obtained using the variance attribute from slices of the amplitude volume F3 Block [8] after the execution of the oriented filtering described by Daber *et.al* [9].

Since there were no public code used in either one of them, the results from the method presented by Pedersen *et al.* [2, 3] were obtained from an execution of the *Ant Tracking*[®] algorithm by an experienced Geologist, while the results shown for Zhao *et al.* [1] were obtained from our implementation of their article.

Our method, illustrated on Figures 2(b) and 3(b), has a significantly reduced amount of noise when compared to the others. The fault edges present fewer discontinuities and less false positives, allowing for an easier extraction.

5 Conclusion

This article proposes ways to improve upon methods that use ACO to enhance seismic fault attributes. Among our contributions are the pheromone deposition

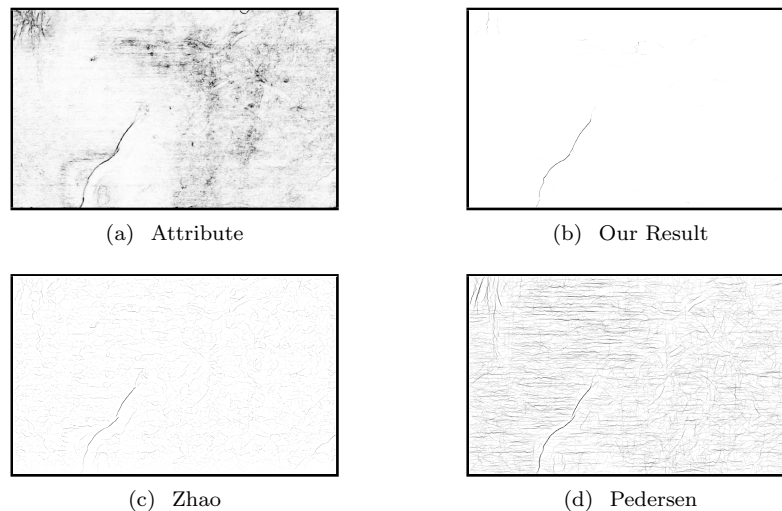


Fig. 3: F3Block's timeslice 404

proportional to the Euclidean distance, the evaporation of the pheromone providing noise suppression and the ant distribution in different gamma factors in order to achieve a good coverage along with good concentration of ants.

As can be seen by the results, our method was capable of delivering cleaner and sharper fault edges. These characteristics are essential if we were to attempt an automatic extraction of fault surfaces across multiple slices.

References

- [1] Junsheng Zhao and Sam Z. Sun. Automatic fault extraction using a modified ant-colony algorithm. *Journal of Geophysics and Engineering*, 10(2):025009+, April 2013.
- [2] SI Pedersen, T Skov, T Randen, and L Sønneland. Automatic Fault Extraction Using Artificial Ants. 2005.
- [3] Stein Inge Pedersen. Image feature extraction, April 10 2007. US Patent 7,203,342.
- [4] Marcos Machado. *Geração de Malhas de Falhas em Dados Sísmicos por Aprendizado Competitivo*. PhD thesis, PUC-Rio, DI, Rio de Janeiro, Brasil, março 2008.
- [5] AM Bazen and SH Gerez. Directional field computation for fingerprints based on the principal component analysis of local gradients. In *ProRISC2000*, pages 215–222, 2000.
- [6] Jack E Bresenham. Algorithm for computer control of a digital plotter. *IBM Systems journal*, 4(1):25–30, 1965.
- [7] John Canny. A computational approach to edge detection. *Pattern Analysis and Machine Intelligence, IEEE Transactions on*, (6):679–698, 1986.
- [8] Opendtect. Open Seismic Repository Main / Netherlands Offshore F3 Block, 2013. [Online; accessed 14-May-2014].
- [9] R. Daber, A. Aqrabi, and Schlumberger Limited. *Petrel 2010: Interpreter's Guide to Seismic Attributes*. Schlumberger, 2010.